

This is the accepted manuscript made available via CHORUS. The article has been published as:

## Separable representation of energy-dependent optical potentials

L. Hlophe and Ch. Elster

Phys. Rev. C **93**, 034601 — Published 3 March 2016

DOI: [10.1103/PhysRevC.93.034601](https://doi.org/10.1103/PhysRevC.93.034601)

# Separable Representation of energy-dependent Optical Potentials

L. Hlophe\* and Ch. Elster†

*Institute of Nuclear and Particle Physics, and Department of Physics and Astronomy, Ohio University, Athens, OH 45701*

(Dated: February 15, 2016)

**Background:** One important ingredient for many applications of nuclear physics to astrophysics, nuclear energy, and stockpile stewardship are cross sections for reactions of neutrons with rare isotopes. Since direct measurements are often not feasible, indirect methods, e.g. (d,p) reactions, should be used. Those (d,p) reactions may be viewed as three-body reactions and described with Faddeev techniques.

**Purpose:** Faddeev equations in momentum space have a long tradition of utilizing separable interactions in order to arrive at sets of coupled integral equations in one variable. Optical potentials representing the effective interactions in the neutron (proton) nucleus subsystem are usually non-Hermitian as well as energy-dependent. Potential matrix elements as well as transition matrix elements calculated with them must fulfill the reciprocity theorem. The purpose of this paper is to introduce a separable, energy-dependent representation of complex, energy-dependent optical potentials that fulfill reciprocity exactly.

**Methods::** Momentum space Lippmann-Schwinger integral equations are solved with standard techniques to obtain the form factors for the separable representation.

**Results:** Starting from a separable, energy-independent representation of global optical potentials based on a generalization of the Ernst-Shakin-Thaler (EST) scheme, a further generalization is needed to take into account the energy dependence. Applications to  $n+^{48}\text{Ca}$ ,  $n+^{208}\text{Pb}$ , and  $p+^{208}\text{Pb}$  are investigated for energies from 0 to 50 MeV with special emphasis on fulfilling reciprocity.

**Conclusions:** We find that the energy-dependent separable representation of complex, energy-dependent phenomenological optical potentials fulfills reciprocity exactly. In addition, taking into account the explicit energy dependence slightly improves the description of the  $S$  matrix elements.

PACS numbers: 24.10.Ht, 25.10.+s, 25.40.Dn, 25.40.Cm

---

\* lh421709@ohio.edu

† elster@ohio.edu

## I. INTRODUCTION

Deuteron induced nuclear reactions are attractive from an experimental as well as theoretical point of view to probe the structure of exotic nuclei. For example, carried out in inverse kinematics, (d,p) or (d,n) reactions prove useful for extracting neutron or proton capture rates for unstable nuclei of astrophysical relevance (see e.g. [1]). From a theoretical perspective (d,p) and (d,n) reactions are attractive, since the scattering problem may be viewed as an effective three-body problem [2]. One of the most challenging aspects of solving the three-body problem for nuclear reactions is the repulsive Coulomb interaction between the nucleus and the proton. While for very light nuclei, exact calculations of (d,p) reactions based on momentum-space Faddeev equations in the Alt-Grassberger-Sandhas (AGS) [3] formulation can be carried out [4] by using a screening and renormalization procedure [5, 6], this technique leads to increasing technical difficulties when moving to computing (d,p) reactions with heavier nuclei [7]. Therefore, a new formulation of the Faddeev-AGS equations, which does not rely on a screening procedure, was presented in Ref. [8]. Here the Faddeev-AGS equations are cast in a momentum-space Coulomb-distorted partial-wave representation instead of the plane-wave basis. Thus all operators, specifically the interactions in the two-body subsystems must be evaluated in the Coulomb basis, which is a nontrivial task (performed recently for the neutron-nucleus interaction [9]). The formulation of Ref. [8] requires the interactions in the subsystems to be of separable form.

Separable representations of the forces between constituents forming the subsystems in a Faddeev approach have a long tradition, specifically when considering the nucleon-nucleon (NN) interaction (see e.g. [10–12]) or meson-nucleon interactions [13, 14]. Here the underlying potentials are Hermitian, and a scheme for deriving separable representations suggested by Ernst-Shakin-Thaler [15] (EST) is well suited, specifically when working in momentum space. It has the nice property that the on-shell and half-off-shell transition matrix elements of the separable representation are exact at predetermined energies, the so-called EST support points. However, when dealing with neutron-nucleus (nA) or proton-nucleus (pA) phenomenological optical potentials, which are in general complex to account for absorptive channels that are not explicitly treated, as well as energy-dependent, extensions of the EST scheme have to be made.

The generalization to non-Hermitian potentials which ensures that the potential as well as the transition matrix elements fulfill the reciprocity theorem is given in Ref. [16]. Essential for this extension is the use of incoming as well as outgoing scattering wave functions when setting up the EST scheme. For a separable representation of pA optical potentials an EST construction has to be carried out in the basis of momentum space Coulomb functions instead of plane waves [17]. Refs. [16] and [17] show that separable representations of phenomenological global optical potentials of Woods-Saxon type can readily be obtained for light ( $^{12}\text{C}$ ) as well as heavy ( $^{208}\text{Pb}$ ) nuclei.

Strictly speaking, the EST representation of Ref. [15] has the drawback that its underlying assumptions rely on the energy independence of the original potential. Unfortunately, today's phenomenological global optical potentials are all energy-dependent. This drawback has been recognized by B.C. Pearce [18], who showed how the energy dependence of Hermitian potentials can be accommodated in the EST scheme. Those suggestion were implemented for pion-nucleon interactions in Refs. [19, 20].

In Section II we concentrate on nucleon-nucleus scattering and show how the extension of Pearce [18] to explicitly accommodate energy dependence in the EST scheme can be combined with our previous extension to non-Hermitian potentials [16]. Here we specifically give the additional momentum-space terms that need to be calculated. In Section II B we show that those additional terms mainly affect the off-shell behavior of partial-wave transition matrix elements, and that only when taking into account the energy dependence reciprocity is fulfilled exactly. We also study select partial-wave S-matrix elements for  $n+^{48}\text{Ca}$  and  $n+^{208}\text{Pb}$ , where we show that for on-shell quantities the explicit energy dependence has very little effect. In Section III we show how this energy-dependent formulation of a separable representation can be employed for proton-nucleus scattering, and present results for  $p+^{208}\text{Pb}$ , a case where the Coulomb interaction is strong. Since taking into account the energy dependence explicitly may considerably increase the computational effort when using this separable representation, we also study the possibility of interpolating on the energy dependence of the optical potential. Finally, we summarize our findings in Section IV.

## II. ENERGY-DEPENDENT NEUTRON-NUCLEUS OPTICAL POTENTIALS

### A. Formal Considerations

While the pioneering work by Ernst, Shakin and Thaler [15] constructed separable representations of Hermitian potentials, optical potentials that describe the scattering of neutrons and protons from nuclei are in general complex as well as energy-dependent. In Ref. [16] the EST scheme was extended to complex potentials. We briefly recall the most important features, namely that a separable representation for a complex, energy-independent potential  $U_l$  in a

fixed partial wave of orbital angular momentum  $l$  is given by [16]

$$u_l = \sum_{ij} U_l |\psi_{l,i}^+\rangle \lambda_{ij}^{(l)} \langle \psi_{l,j}^- | U_l, \quad (1)$$

where  $|\psi_{l,i}^+\rangle$  is a solution of the Hamiltonian  $H = H_0 + U_l$  with outgoing boundary conditions at energy  $E_i$ , and  $|\psi_{l,i}^-\rangle$  is a solution of the Hamiltonian  $H = H_0 + U_l^*$  with incoming boundary conditions. We refer to the energies  $E_i$  as EST support points. The free Hamiltonian  $H_0$  has eigenstates  $|k_i\rangle$  with  $k_i^2 = 2\mu E_i$ ,  $\mu$  being the reduced mass of the neutron-nucleus system. The matrix  $\lambda_{ij}^{(l)}$  is constrained by the conditions

$$\begin{aligned} \delta_{kj} &= \sum_i \langle \psi_{l,k}^- | U_l | \psi_{l,i}^+ \rangle \lambda_{ij}^{(l)} \\ \delta_{ik} &= \sum_j \lambda_{ij}^{(l)} \langle \psi_{l,j}^- | U_l | \psi_{l,k}^+ \rangle, \end{aligned} \quad (2)$$

where the subscript  $i = 1 \dots N$  indicates the rank of the separable potential. The two constraints of Eq. (2) on  $\lambda_{ij}^{(l)}$  ensure that at the EST support points  $E_i$ , both the original  $U$  and the separable potential  $u$ , yield identical wavefunctions or half-shell  $t$  matrices. The corresponding separable  $t$  matrix takes the form

$$t_l(E) = \sum_{ij} U_l |\psi_{l,i}^+\rangle \tau_{ij}^{(l)}(E) \langle \psi_{l,j}^- | U_l \quad (3)$$

with

$$\left( \tau_{ij}^{(l)}(E) \right)^{-1} = \langle \psi_{l,i}^- | U_l - U_l g_0(E) U_l | \psi_{l,j}^+ \rangle. \quad (4)$$

Here  $g_0(E) = (E - H_0 + i\varepsilon)^{-1}$  is the free propagator. The form factors are given as half-shell  $t$ -matrices

$$T_l(E_i) |k_i\rangle \equiv U_l | \psi_{l,i}^+ \rangle, \quad (5)$$

and are obtained through solving a momentum space Lippmann-Schwinger (LS) equation.

Given a time reversal operator  $\mathcal{K}$ , the optical potential  $U$  satisfies

$$\mathcal{K} U \mathcal{K}^{-1} = U^\dagger, \quad (6)$$

so that the corresponding  $t$ -matrix fulfills reciprocity. We therefore require that its EST separable representation  $u$  preserves this property. A proof that the separable potential defined in Eqs. (1) and (3) obeys the relation  $\mathcal{K} u \mathcal{K}^{-1} = u^\dagger$  is provided in Ref. [16] for the rank-1 case. Generalization of the proof to a higher rank requires that the matrix  $\lambda_{ij}^{(l)}$  be symmetric in the indices  $(i, j)$ . If the potential is energy-independent this symmetry of  $\lambda_{ij}^{(l)}$  is evident when examining the constraints of Eq. (2).

However, when applying the same formulation to an energy-dependent potential  $U(E)$ , one obtains

$$u_l = \sum_{ij} U_l(E_i) |\psi_{l,i}^+\rangle \lambda_{ij}^{(l)} \langle \psi_{l,j}^- | U_l(E_j), \quad (7)$$

with the constraints

$$\begin{aligned} \delta_{kj} &= \sum_i \langle \psi_{l,k}^- | U_l(E_i) | \psi_{l,i}^+ \rangle \lambda_{ij}^{(l)} \\ \delta_{ik} &= \sum_j \lambda_{ij}^{(l)} \langle \psi_{l,j}^- | U_l(E_j) | \psi_{l,k}^+ \rangle. \end{aligned} \quad (8)$$

Omitting the partial wave index  $l$  the two constraints on  $\lambda$  can be written in matrix form

$$\mathcal{U}^t \lambda = \mathbf{1} = \lambda \mathcal{U}, \quad (9)$$

with

$$\mathcal{U}_{ij} = \langle \psi_i^- | U(E_i) | \psi_j^+ \rangle. \quad (10)$$

For a separable potential of rank  $N > 1$  the matrix  $\mathcal{U}_{ij}$  is not symmetric in the indices  $i$  and  $j$ , which leads to an asymmetric matrix  $\lambda$  and thus a  $t$  matrix which violates reciprocity. Therefore, a different approach must be taken in order to construct separable representations for energy-dependent potentials. Here we note that although the potential  $u$  contains some of the energy dependence of  $U(E)$  through the form factors, it has no explicit energy dependence. Henceforth we will refer to this separable construction as the energy-independent EST representation.

A separable expansion for energy-dependent Hermitian potentials was suggested by B.C. Pearce [18]. This suggestion can also be applied to complex potentials by using the insights already gained in [16]. In analogy, we define the EST separable representation for complex energy-dependent potentials (eEST) by allowing an explicit energy dependence of the coupling matrix elements  $\lambda_{ij}$ .

$$u(E) = \sum_{ij} U(E_i) |\psi_i^+\rangle \lambda_{ij}(E) \langle \psi_j^- | U(E_j), \quad (11)$$

where the partial wave index  $l$  has been omitted for simplicity. In order to obtain a constraint on the matrix  $\lambda(E)$ , we require that the matrix elements of the potential  $U(E)$  and its separable form  $u(E)$  between the states  $|\psi_i^+\rangle$  be the same at all energies  $E$ . This condition ensures that the potentials  $U(E)$  and  $u(E)$  yield identical wavefunctions at the EST support points, just like in the energy-independent EST scheme. The constraints on  $\lambda_{ij}(E)$  become

$$\begin{aligned} \langle \psi_m^- | U(E) | \psi_n^+ \rangle &= \langle \psi_m^- | u(E) | \psi_n^+ \rangle \\ &= \sum_i \langle \psi_m^- | U(E_i) | \psi_i^+ \rangle \lambda_{ij}(E) \langle \psi_j^- | U(E_j) | \psi_n^+ \rangle. \end{aligned} \quad (12)$$

The corresponding separable  $t$ -matrix then takes the form

$$t(E) = \sum_{ij} U(E_i) |\psi_i^+\rangle \tau_{ij}(E) \langle \psi_j^- | U(E_j). \quad (13)$$

Substituting Eqs. (11)–(13) into the LS equation leads to the constraint on the matrix  $\tau(E)$  such that

$$R(E) \cdot \tau(E) \equiv \mathcal{M}(E), \quad (14)$$

where

$$R_{ij}(E) = \langle \psi_i^- | U(E_i) | \psi_j^+ \rangle - \sum_n \mathcal{M}_{in}(E) \langle \psi_n^- | U(E_n) g_0(E) U(E_j) | \psi_j^+ \rangle, \quad (15)$$

with

$$\mathcal{M}_{in}(E) \equiv [\mathcal{U}^e(E) \cdot \mathcal{U}^{-1}]_{in}, \quad (16)$$

where the matrix elements of  $\mathcal{U}$  are defined in Eq. (10). We want to point out that, for energy-independent potentials, the matrix  $\mathcal{M}(E)$  simply is the unit matrix. For further evaluating these matrix elements in momentum space, we express

$$\mathcal{U}_{ij}^e(E) \equiv \langle \psi_i^- | U(E) | \psi_j^+ \rangle, \quad (17)$$

in terms of the potential and the half-shell  $t$  matrix so that

$$\begin{aligned} \mathcal{U}_{ij}^e(E) &= \langle k_i | U(E) | k_j \rangle + \langle \psi_i^- | U(E_i) g_0(E_i) U(E) | k_j \rangle + \langle k_i | U(E) g_0(E_j) U(E_j) | \psi_j^+ \rangle \\ &\quad + \langle \psi_i^- | U(E_i) g_0(E_i) U(E) g_0(E_j) U(E_j) | \psi_j^+ \rangle, \\ &= \langle k_i | U(E) | k_j \rangle + \langle k_i | T(E_i) g_0(E_i) U(E) | k_j \rangle + \langle k_i | U(E) g_0(E_j) T(E_j) | k_j \rangle \\ &\quad + \langle k_i | T(E_i) g_0(E_i) U(E) g_0(E_j) T(E_j) | k_j \rangle. \end{aligned} \quad (18)$$

Inserting a complete set of momentum eigenstates leads to the explicit expression for  $\mathcal{U}_{ij}^e(E)$ ,

$$\begin{aligned} \mathcal{U}_{ij}^e(E) &= U(k_i, k_j, E) + \int_0^\infty dp p^2 T(p, k_i; E_i) g_0(E_i, p) U(p, k_j, E) \\ &\quad + \int_0^\infty dp p^2 U(k_i, p, E) g_0(E_j, p) T(p, k_j; E_j) \end{aligned}$$

$$+ \int_0^\infty dp p^2 \int_0^\infty dp' p'^2 T(p, k_i; E_i) g_0(E_i, p) U(p, p', E) g_0(E_j, p') T(p', k_j; E_j), \quad (19)$$

where  $g_0(E, p) = [E - p^2/2\mu + i\varepsilon]^{-1}$ . For the evaluation of  $\mathcal{U}_{ij}^e(E)$  for all energies  $E$  within the relevant energy regime, we need the form factors  $T(p', k_j; E_j)$  at the specified EST support points as well as the matrix elements of the potential  $U(p', p, E)$  at all energies.

### B. Energy-independent EST Scheme versus eEST Separable Representation

For studying the properties of the energy-dependent separable representation eEST, we consider elastic scattering of neutrons off  $^{48}\text{Ca}$  and  $^{208}\text{Pb}$  from 0 to 50 MeV. We employ the Chapel Hill (CH89) phenomenological global optical potential [21] in all calculations. First, we investigate the symmetry properties of the off-shell partial wave  $t$  matrix  $t_l^j(k', k; E)$  in the eEST separable representation and contrast them with the ones obtained via the energy independent EST scheme. To do so, we adopt the same energy support points for the both EST separable representations. Fig. 1 shows the off-shell  $t$  matrix  $t_{l=6}^{j=13/2}(k', k; E)$  as function of the off-shell momenta  $k$  and  $k'$  for the  $n+^{48}\text{Ca}$  system at  $E_{lab} = 16$  MeV. The real and imaginary parts of the off-shell  $t$  matrix evaluated with the CH89 optical potential are shown in panels (a) and (d). The energy-independent EST calculation is given in panels (b) and (e), while the eEST separable representation is depicted in panels (c) and (f). We observe that the structure of the off-shell separable  $t$  matrix appears to be the same for both the energy-dependent and energy-independent representations. The high momentum components which are visible in the CH89 off-shell  $t$  matrix are projected out by both separable representations. This is a general feature of the EST separable representation. As further example, we consider neutron scattering off the much heavier  $^{208}\text{Pb}$  nucleus as depicted in Fig. 2 for the  $l = 0$  partial wave. In both figures the separable off-shell  $t$ -matrices appear to be symmetric around the  $k = k'$  line. However we know from the formal considerations in the previous section that the energy-independent EST scheme does not fully satisfy reciprocity and therefore should yield an asymmetric off-shell  $t$  matrix in  $k$  and  $k'$ . In order to carry out a more careful analysis of the symmetry properties of the  $t$ -matrix we define an asymmetry

$$\Delta t_l^j(k', k; E) = \frac{\left| t_l^j(k', k; E) - t_l^j(k, k'; E) \right|}{\frac{1}{2} \left| t_l^j(k', k; E) + t_l^j(k, k'; E) \right|}, \quad (20)$$

representing the relative difference between the off-shell  $t$  matrix and its transpose. For a completely symmetric off-shell  $t$  matrix this asymmetry should be exactly zero. In Fig. 3 we show the asymmetry  $\Delta t_{l=6}^{j=13/2}(k', k; E)$  for  $n+^{48}\text{Ca}$  scattering for the energy-independent EST separable representation at  $E_{lab} = 16$  MeV (panel (a)) and 40 MeV (panel (b)). The asymmetry is either zero or very small close to the  $k = k'$  axis and at small momenta. However, away from this region it can become quite large. For the eEST separable representation the asymmetry is exactly zero everywhere as expected, and thus is not shown. This shows that in order to exactly fulfill reciprocity the eEST separable representation must be employed.

So far we only considered off-shell properties of the eEST separable representation. The next question is whether there is an on-shell difference between the energy-dependent and energy-independent schemes. As a measure of the quality of the eEST separable representation, we define the relative error of the real part of the  $S$  matrix as

$$\text{relative error} = \left| \frac{\text{Re } S_l^j(E)^{orig} - \text{Re } S_l^j(E)^{sep}}{S_l^j(E)^{orig}} \right|, \quad (21)$$

where  $S_l^j(E)^{orig}$  is the partial wave  $S$  matrix calculated from the CH89 potential and  $S_l^j(E)^{sep}$  the one obtained from the separable representation. The real part of the  $n+^{48}\text{Ca}$   $S$  matrix for  $l = 6$  and  $j = 13/2$  together with the corresponding relative error is depicted in panels (a) and (b) of Fig. 4. The  $S$  matrix obtained from the CH89 phenomenological optical potential is shown by the dash-dotted line while the energy-independent and eEST separable representations are depicted by dashed and solid lines. The relative error is indicated by upward triangles for the EST separable representation and by circles for the eEST scheme. There is good agreement between the CH89  $S$  matrix and both separable representations. However the eEST separable representation describes the  $S$  matrix slightly better than its energy-independent counterpart since it incorporates more of the energy dependence of the original potential. This is visible for energies around  $E_{lab} = 37$  MeV, where the relative error is dominated by the separable approximation. However, the energy-independent EST representation can always be improved by adding

an extra support point, i.e. increasing the rank. This means that the observations made in Ref. [16] concerning on shell properties of the energy-independent EST representation apply to the eEST separable representation as well. The main reason for adopting the eEST separable representation is that it yields exact reciprocity.

### III. APPLICATION TO PROTON-NUCLEUS OPTICAL POTENTIALS

#### A. Formal Considerations

The proton-nucleus potential consists of the point Coulomb force,  $V^c$ , together with a short-ranged nuclear as well as a short-ranged Coulomb interaction representing the charge distribution of the nucleus, which we refer to as  $U^s(E)$ . While the point Coulomb potential has a simple analytical form, an optical potential is employed to model the short-range nuclear potential. The extension of the energy-independent EST separable representation to proton-nucleus optical potentials was carried out in Ref. [17]. In that work it was shown that the form factors of the separable representation are solutions of the LS equation in the Coulomb basis, and that they are obtained using methods introduced in Refs. [22, 23]. It was also demonstrated that the extension of the energy-independent EST separable representation scheme to proton-nucleus scattering involves two steps. First, the nuclear wavefunctions  $|\psi_{l,i}^{(+)}\rangle$  are replaced by Coulomb-distorted nuclear wavefunctions  $|\psi_{l,i}^{sc (+)}\rangle$ . Second, the free resolvent  $g_0(E)$  is replaced by the Coulomb Green's function,  $g_c(E) = (E - H_0 - V^c + i\varepsilon)^{-1}$ . As demonstrated in Section II, in order to fulfill reciprocity, an energy-dependent separable representation must be adopted. This is accomplished by generalizing the eEST scheme to proton-nucleus scattering analogous to the extension of the energy-independent EST scheme presented in Ref. [17]. Thus applying the two steps outlined above to the eEST scheme yields the separable Coulomb-distorted nuclear  $t$ -matrix

$$t_l^{sc}(E) = \sum_{i,j} U_l^s(E_i) |\psi_{l,i}^{sc (+)}\rangle \tau_{ij}^{c,l}(E) \langle \psi_{l,j}^{sc (-)} | U_l^s(E_j). \quad (22)$$

Here  $|\psi_{l,i}^{sc (+)}\rangle$  are solutions corresponding to  $U_l^s(E_i)$  in the Coulomb basis with outgoing boundary conditions, and  $|\psi_{l,i}^{sc (-)}\rangle$  are solutions corresponding to  $(U_l^s)^*(E_i)$  with incoming boundary conditions. Upon suppressing the index  $l$  we obtain a constraint similar to Eq. (14),

$$R^c(E) \cdot \tau^c(E) = \mathcal{M}_{ij}^c(E), \quad (23)$$

with the matrix elements of  $R^c(E)$  satisfying

$$R_{ij}^c(E) = \langle \psi_i^{sc (-)} | U^s(E_i) | \psi_j^{sc (+)} \rangle - \sum_i \mathcal{M}_{in}^c(E) \langle \psi_n^{sc (-)} | U^s(E_n) g_c(E) U^s(E_j) | \psi_j^{sc (+)} \rangle. \quad (24)$$

The matrix  $\mathcal{M}^c(E)$  is the Coulomb distorted counterpart of  $\mathcal{M}(E)$  of Eq. (16), and is defined as

$$\mathcal{M}_{in}^c(E) = [\mathcal{U}^{e,sc}(E) \cdot (\mathcal{U}^{sc})^{-1}]_{in}, \quad (25)$$

with

$$\begin{aligned} \mathcal{U}_{ij}^{sc} &\equiv \langle \psi_i^{sc (-)} | U^s(E_i) | \psi_j^{sc (+)} \rangle, \\ \mathcal{U}_{ij}^{e,sc}(E) &\equiv \langle \psi_{ki}^{sc (-)} | U^s(E) | \psi_{kj}^{sc (+)} \rangle. \end{aligned} \quad (26)$$

If the potential is energy-independent the matrix  $\mathcal{M}^c(E)$  becomes a unit matrix just like  $\mathcal{M}(E)$ .

For evaluating  $\mathcal{U}_{ij}^{e,sc}(E)$  one can proceed analogously to Eq. (18) and finally arrive at an expression similar to Eq. (19), namely

$$\begin{aligned} \mathcal{U}_{ij}^{e,sc}(E) &= U^{sc}(k_i, k_j, E) + \int_0^\infty dp p^2 T^{sc}(p, k_i; E_i) g_c(E_i, p) U^{sc}(p, k_j, E) \\ &\quad + \int_0^\infty dp p^2 U^{sc}(k_i, p, E) g_c(E_j, p) T^{sc}(p, k_j; E_j) \\ &\quad + \int_0^\infty dp p^2 \int_0^\infty dp' p'^2 T^{sc}(p, k_i; E_i) g_c(E_i, p) U^{sc}(p, p', E) g_c(E_j, p') T^{sc}(p', k_j; E_j). \end{aligned} \quad (27)$$



Since all matrix elements are evaluated in the Coulomb basis, the Coulomb Green's function has the same form as the free Green's function in the calculations. The matrix elements of the short-ranged potential in the basis of Coulomb scattering states  $U^{sc}(k_i, k_j, E) \equiv \langle \phi_{k_i}^{c(+)} | U^s | \phi_{k_j}^{c(+)} \rangle$  are calculated in the same fashion as the ones in Eq. (9) of Ref. [17]. The Coulomb distorted short-ranged half-shell  $t$  matrix  $T^{sc}(p, k_i, E_i)$  is then evaluated using Eq. (6) of the same reference.

### B. Energy-independent EST Scheme versus eEST Separable Representation

In this section the generalization of the eEST separable representation is applied to elastic scattering of protons off  $^{208}\text{Pb}$ . The short-range interaction  $U^s(E)$  is comprised of the CH89 global optical potential [21] and a short-ranged Coulomb potential, representing the charge distribution of the  $^{208}\text{Pb}$  nucleus as used for the calculations of Ref. [17]. As in Section II B, we first concentrate on the off-shell  $t$  matrices to verify that the energy dependent eEST representation for charged particles fulfills reciprocity exactly. Since the Coulomb distortion of plane wave states is most pronounced in low partial waves, the  $s$ -wave off-shell  $t$  matrix is examined. Panels (a) and (d) of Fig. 5 depict the real and imaginary parts of the off-shell  $t$  matrix for the  $p+^{208}\text{Pb}$  system calculated with the CH89 potential. Comparing those panels to the corresponding ones in Fig. 2 shows that the attractive part of the  $n+^{208}\text{Pb}$   $t$  matrix at low momenta  $k$  and  $k'$  is absent in the  $p+^{208}\text{Pb}$   $t$  matrix, indicating that the Coulomb interaction dominates here. Since we already showed in Figs. 1 and 2 that there is no visual difference in the off-shell  $t$  matrices when comparing the energy-independent and energy-dependent separable representation, we only show the eEST separable representation in Fig. 5 in panels (b) and (d). As already observed for the neutron off-shell  $t$  matrices of Figs. 1 and 2, the separable representation projects out the high momentum components.

The asymmetry calculated according to Eq. (20) for the energy-independent separable representation is illustrated in panel (c) while panel (f) depicts the asymmetry for the eEST separable representation. The latter shows an exact zero. As was the case for the  $n+^{208}\text{Pb}$  and  $n+^{48}\text{Ca}$  off-shell  $t$  matrices, the eEST representation generalized for proton scattering is completely symmetric in the momenta  $k$  and  $k'$ , leading to a zero asymmetry. This is not the case for the energy independent EST generalization of Ref. [17], which is shown in panel (c). This demonstrates that also the eEST representation of proton-nucleus optical potentials fulfills reciprocity exactly.

Next we examine the on-shell properties for proton scattering from  $^{208}\text{Pb}$ , and concentrate on the  $l = 0$ ,  $j = 1/2$  partial wave. To keep the relative error defined in Eq. (21) below 2% in the energy range from 0 to 50 MeV it is necessary to employ a rank-5 representation of the CH89 optical potential in the lower partial waves [17] even in the eEST scheme. In this case the error is dominated by numerical interpolation when calculating the separable representation. To compare the eEST scheme to its energy-independent counterpart, we artificially lower the accuracy of the separable expansion to rank-4. This leads to a relative error that is dominated by the quality of the separable representation over the energy range under consideration. In panel (a) of Fig. 6 the  $S$  matrix elements obtained from the CH89 potential are depicted together with their EST and eEST rank-4 separable representations in the energy range from 0 to 50 MeV. The relative errors with respect to the CH89 result give a more detailed insight and are shown for the two different schemes in panel (b) of the same figure as filled circles for eEST and upward triangles for EST scheme. As already observed in Section II B, the eEST scheme yields a better representation of the  $S$  matrix between 20 and 35 MeV than the EST representation. By increasing the rank to a rank-5 representation, both representations can be improved for this energy interval.

### C. Approximation to the Energy Dependence

The matrix elements  $\mathcal{U}_{ij}^{e,sc}(E)$  are evaluated according to Eq. (27). Additional numerical work is required to compute the Coulomb distorted short-ranged potential  $U^{sc}(k', k, E)$  at each energy  $E$ . This makes the implementation of the eEST separable representation computationally more involved compared to the energy-independent scheme. In cases where calculating the potential  $U^s(E)$  in the plane wave basis is already time consuming, employing the eEST scheme may become prohibitively costly. Therefore, it is worthwhile exploring if the eEST can be modified in such a way that the potential  $U^s(E)$  is calculated only at a specified fixed set of energies.

In general the energy dependence of optical potentials is smooth and thus one may think of interpolating  $\mathcal{U}^{e,sc}(E)$  on the energy variable. We tested such an interpolation scheme starting by adopting the energies of the support points at which the potential  $U^s(E)$  is already calculated as grid points for an interpolation with Cubic Hermite splines [25]. The  $S$  matrix elements evaluated using the interpolated eEST scheme is shown by a dash-dot-dotted line in panel (a) of Fig. 6, while the relative error is indicated by crosses in panel (b). As the figure illustrates, using an interpolation to approximate the energy dependence of the CH89 potential yields the same relative error as the exact



eEST calculation. This means, that the EST support points can already provide a good interpolation grid. However, in cases with a more intricate energy dependence or if the distance between support points is much larger, it may turn out to be necessary to add a few more energy points.

The use of an energy interpolation greatly reduces the numerical effort needed to evaluate  $\mathcal{U}^{e,sc}(E)$  on the energy grid from 0 to 50 MeV. The gain in computation time decreases with the number of interpolation points but increases with the density of the energy grid. In the calculations presented here, there are four interpolation points and the energy grid consists of 100 points. Employing an interpolation to approximate the matrix elements  $\mathcal{U}_{ij}^{e,sc}(E)$  reduces the computational effort by a factor of 23. As pointed out in Section III B, a more accurate separable representation of the s-wave  $S$  matrix for the  $p+^{208}\text{Pb}$  system requires five EST support points. For this case there are five interpolation points and the computation time is decreased by a factor of 18.

#### IV. SUMMARY AND CONCLUSIONS

In this work we introduce an explicit energy dependence into our previously developed separable representation of two-body transition matrix elements as well as potentials for nucleon-nucleus [16] and proton-nucleus [17] phenomenological global optical potentials. Those potentials are in general complex and energy-dependent. While on-shell properties like scattering amplitudes and cross sections can be well reproduced by an energy-independent separable representation, for which we generalized the Ernst-Shakin-Thaler [15] (EST) scheme to complex potentials [16], the so obtained fully-off shell separable transition matrix elements fulfill the reciprocity theorem only approximately, specifically when going far off the energy shell. The reason for this behavior lies in the energy dependence of the optical potential for which we construct the separable representation. Specifically, the conditions for the coupling constants posed by the EST construction, Eqs. (2), can not be fulfilled simultaneously when the potential is energy dependent. This insight had already been pointed out in Ref. [18] and the EST scheme was corrected for Hermitian energy-dependent potentials. Picking up these suggestions and applying them to non-Hermitian, energy-dependent optical potentials leads to an explicitly energy-dependent separable expansion, eEST, which fulfills reciprocity exactly.

As specific examples we consider neutron scattering from  $^{48}\text{Ca}$  and  $^{208}\text{Pb}$  described by the Chapel Hill global phenomenological optical potential [21], and demonstrate for two different partial wave channels that the fully off-shell transition matrix is exactly symmetric under the exchange of the off-shell momenta  $k'$  and  $k$ , and thus fulfills reciprocity. For the on-shell condition, we show that an energy-dependent eEST representation of a partial wave  $S$  matrix is slightly superior to its energy-independent EST counterpart. However, one needs to note that any separable representation can always be improved on-shell by increasing its rank, while the symmetry property of the off-shell transition amplitude is not affected by the rank.

Since in a (d,p) reaction calculation one needs the effective interactions in the neutron-nucleus as well as the proton-nucleus subsystem, we extended the energy-independent EST representation from Ref. [17] to an energy-dependent one. The separable representation of the proton-nucleus transition elements is carried out in the basis of Coulomb scattering states. The calculation of required potential matrix elements follows the approach suggested in Refs. [22, 23]. As test case we presented the separable, energy-dependent representation of an  $l = 0$  partial wave off-shell transition amplitude for proton scattering off  $^{208}\text{Pb}$  and demonstrated that it is exactly symmetric under the exchange of the off-shell momenta  $k'$  and  $k$ , thus thus fulfills reciprocity. Similar to the neutron case we also show that the energy-dependent separable representation of the corresponding  $S$  matrix elements are slightly superior to the energy-independent representation for the same rank.

The numerical evaluation of an energy-dependent separable representation is more involved compared to its energy-independent counterpart, since the coupling matrices are now energy dependent and thus need to be evaluated at each energy, not only at the EST support points. Though this is not a particular issue for the phenomenological global optical potentials, it may become computationally expensive for microscopic optical potentials. Therefore we investigated if it is possible to interpolate on the energy variable, which usually exhibits a relatively smooth behavior for optical potentials. We found that, when using the EST support points as interpolation points for an interpolation on the energy with cubic splines, we obtained a separable, energy-dependent representation of identical quality, while considerably reducing the computational effort. Even for cases exhibiting a strong energy dependence of the potential, it will be possible to use an energy interpolation by making the energy grid finer.

Summarizing, by constructing an energy-dependent separable representation of neutron- and proton-optical potentials, one can obtain off-shell transition matrix elements which fulfill the reciprocity theorem exactly. Since off-shell matrix elements are not observables, only reaction calculations can show how severe any consequences, e.g. for three-body observables, small violations of the reciprocity theorem turn out to be.

## ACKNOWLEDGMENTS

This work was performed in part under the auspices of the U. S. Department of Energy under contract No. DE-FG02-93ER40756 with Ohio University. The authors thank F.M. Nunes and I.J. Thompson for thoughtful comments and careful reading of the manuscript.

- 
- [1] R. Kozub, G. Arbanas, A. Adekola, D. Bardayan, J. Blackmon, *et al.*, Phys.Rev.Lett. **109**, 172501 (2012).
  - [2] I. J. Thompson and F. M. Nunes, *Nuclear Reactions for Astrophysics* (Cambridge University Press, 2009).
  - [3] E. Alt, P. Grassberger, and W. Sandhas, Nucl. Phys. B **2**, 167 (1967).
  - [4] A. Deltuva and A. Fonseca, Phys.Rev. **C79**, 014606 (2009).
  - [5] A. Deltuva, A. Fonseca, and P. Sauer, Phys.Rev. **C71**, 054005 (2005).
  - [6] A. Deltuva, A. Fonseca, and P. Sauer, Phys.Rev. **C72**, 054004 (2005).
  - [7] F. Nunes and N. Upadhyay, J. Phys. G: Conf. Ser. **403**, 012029 (2012).
  - [8] A. Mukhamedzhanov, V. Eremenko, and A. Sattarov, Phys.Rev. **C86**, 034001 (2012).
  - [9] N. Upadhyay *et al.* (TORUS Collaboration), Phys. Rev. **C90**, 014615 (2014).
  - [10] J. Haidenbauer and W. Plessas, Phys.Rev. **C27**, 63 (1983).
  - [11] J. Haidenbauer, Y. Koike, and W. Plessas, Phys.Rev. **C33**, 439 (1986).
  - [12] D. Entem, F. Fernandez, and A. Valcarce, J.Phys. **G27**, 1537 (2001).
  - [13] T. Ueda and Y. Ikegami, Prog.Theor.Phys. **91**, 85 (1994).
  - [14] A. Gal and H. Garcilazo, Nucl.Phys. **A864**, 153 (2011).
  - [15] D. J. Ernst, C. M. Shakin, and R. M. Thaler, Phys.Rev. **C8**, 46 (1973).
  - [16] L. Hlophe *et al.* (The TORUS Collaboration), Phys.Rev. **C88**, 064608 (2013).
  - [17] L. Hlophe, V. Eremenko, C. Elster, F. M. Nunes, G. Arbanas, J. E. Escher, and I. J. Thompson, Phys. Rev. **C90**, 061602 (2014).
  - [18] B. Pearce, Phys.Rev. **C36**, 471 (1987).
  - [19] B. C. Pearce and I. R. Afnan, Phys. Rev. **C40**, 220 (1989).
  - [20] T. Y. Saito and J. Haidenbauer, Eur. Phys. J. **A7**, 559 (2000).
  - [21] R. Varner, W. Thompson, T. McAbee, E. Ludwig, and T. Clegg, Phys.Rept. **201**, 57 (1991).
  - [22] C. Elster, L. C. Liu, and R. M. Thaler, J.Phys. **G19**, 2123 (1993).
  - [23] C. R. Chinn, C. Elster, and R. M. Thaler, Phys.Rev. **C44**, 1569 (1991).
  - [24] S. Weppner, R. Penney, G. Diffendale, and G. Vittorini, Phys.Rev. **C80**, 034608 (2009).
  - [25] D. Huber, H. Witala, A. Nogga, W. Gloeckle, and H. Kamada, Few Body Syst. **22**, 107 (1997).

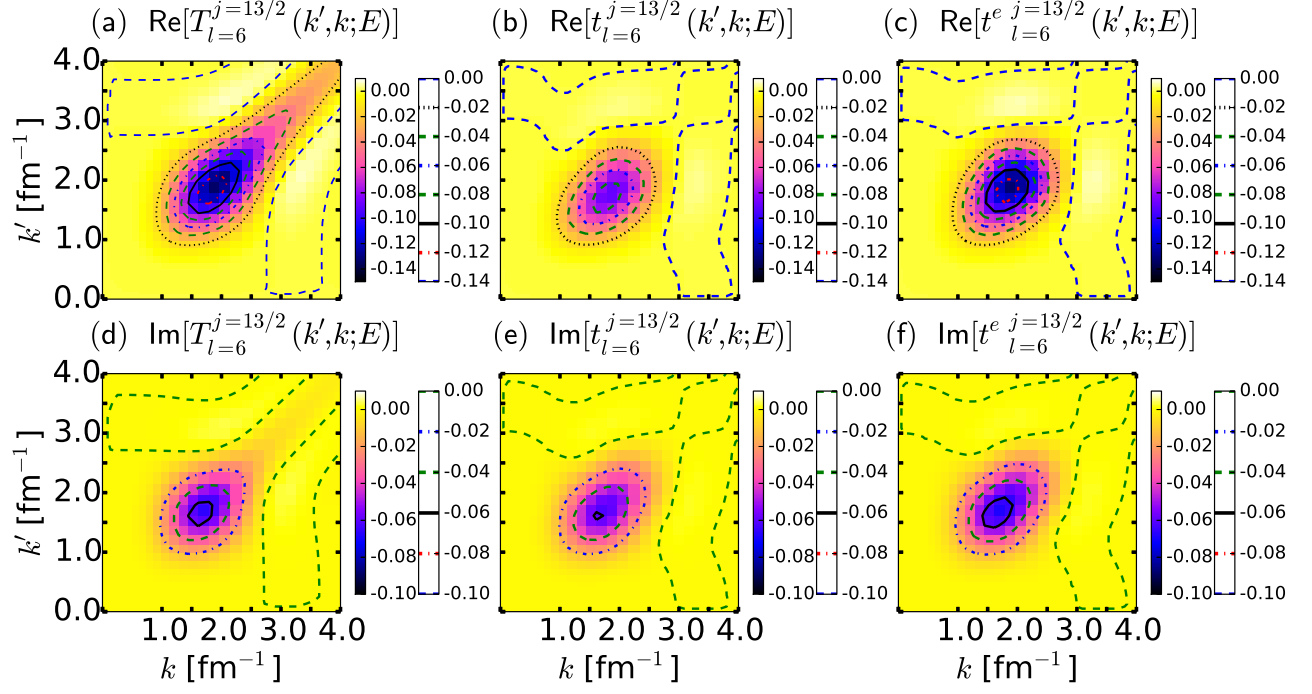


FIG. 1. (Color online) The  $l = 6, j = 13/2$  partial wave off-shell  $t$ -matrix elements,  $t_6(k', k; E)$  in units  $\text{fm}^2$  for the  $n+^{48}\text{Ca}$  system computed at  $E_{lab} = 16$  MeV as function of the off-shell momenta  $k'$  and  $k$ . This energy corresponds to an on shell momentum of  $0.86 \text{ fm}^{-1}$ . The real and imaginary parts of the off-shell  $t$  matrix calculated from the CH89 [21] phenomenological optical potential are shown in panels (a) and (d). The real and imaginary parts of the  $t$  matrix calculated from its energy-independent EST separable representation are shown in panels (b) and (e), while panels (c) and (f) depict the energy-dependent eEST separable representations. The support points for the separable representation are at  $E_{lab}=16, 29$ , and  $47$  MeV.

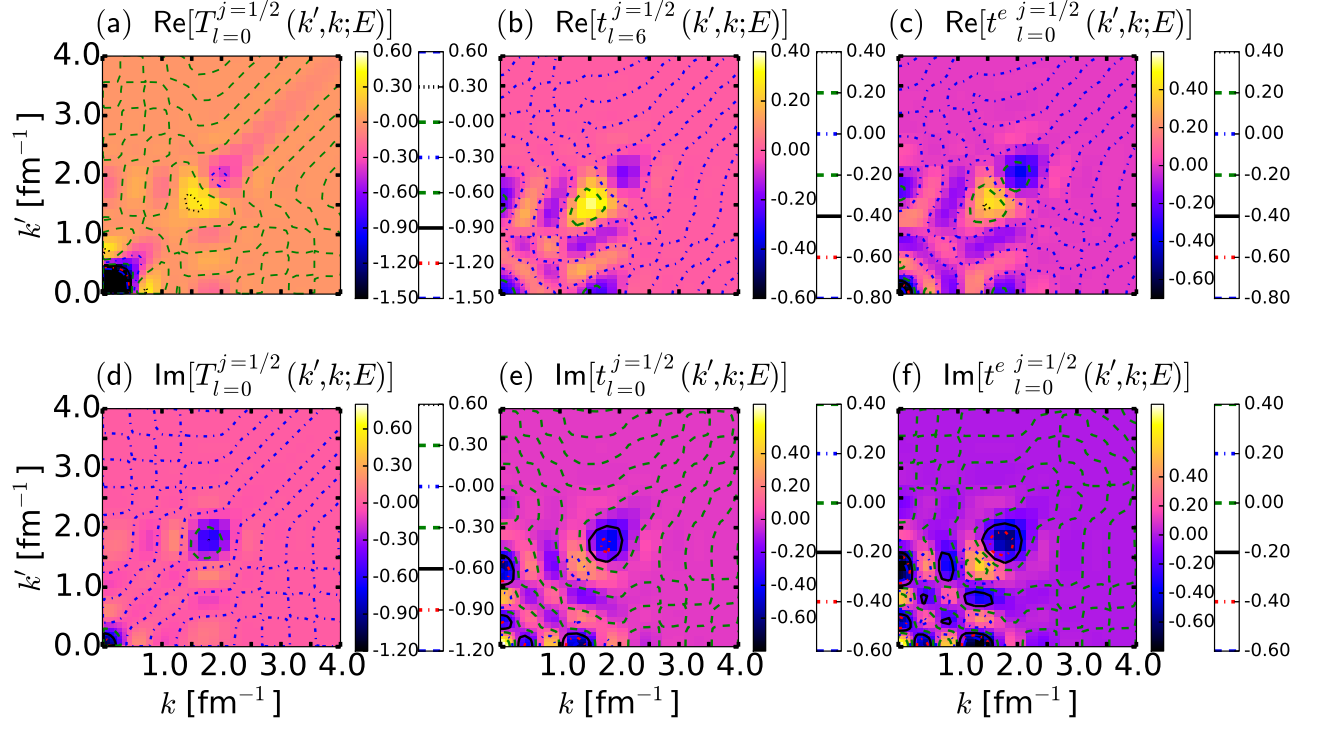


FIG. 2. (Color online) Same as FIG. 1 but for the  $l=0, j=1/2$  partial wave of the  $n+^{208}\text{Pb}$  system at 21 MeV corresponding to an on shell momentum of 1.00 fm $^{-1}$ . The support points for the separable representation are at  $E_{lab}=5, 11, 15, 21$ , and 47 MeV.

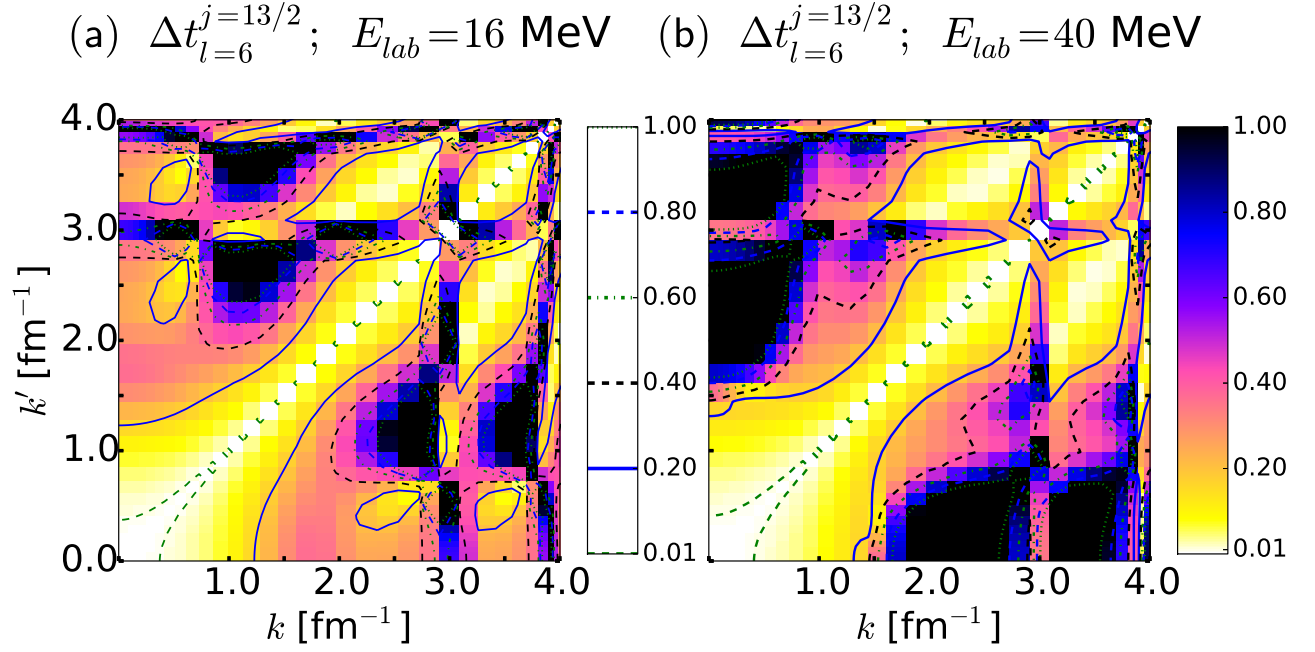


FIG. 3. (color online) The asymmetry  $\Delta t_{l=6}^{j=13/2}(k', k; E)$  for the energy-independent separable representation of the  $t$  matrix obtained from the CH89 [21] phenomenological optical potential as function of the off-shell momenta  $k'$  and  $k$  for the  $n+^{48}\text{Ca}$  system. Panel (a) shows the asymmetry at  $E_{lab} = 16 \text{ MeV}$ , panel (b) at  $40 \text{ MeV}$ . The support points are  $E_{lab} = 16, 29$ , and  $47 \text{ MeV}$ . The on shell momenta are  $0.86 \text{ fm}^{-1}$  and  $1.36 \text{ fm}^{-1}$ .

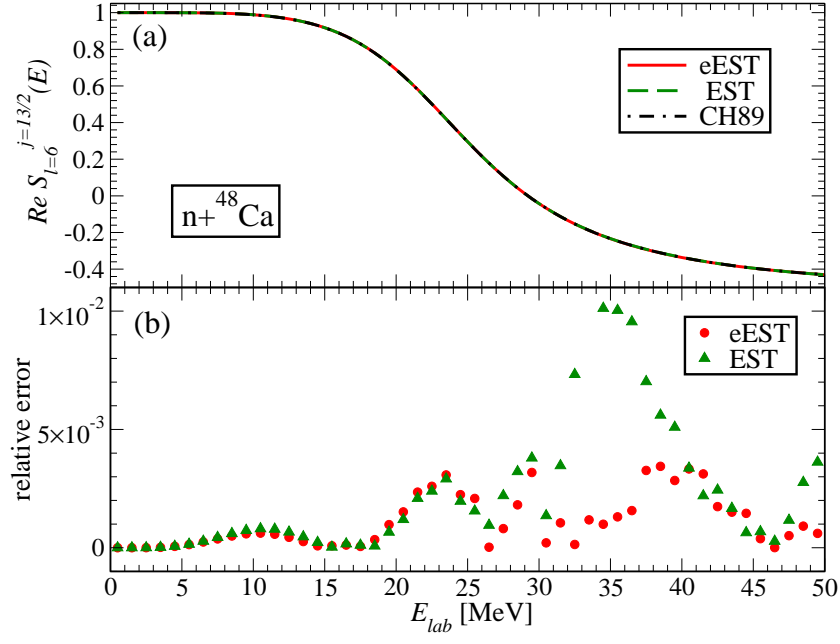


FIG. 4. (color online) The  $S$  matrix elements  $S_{l=6}^{j=13/2}(E)$  for elastic scattering of neutrons from  ${}^{48}\text{Ca}$  in  $l = 6$ ,  $j = 13/2$  partial wave as function of the laboratory energy. The top panel (a) shows the real part of the  $S$  matrix while the bottom panel (b) gives the relative error of the separable representations as defined in Eq. (20). The  $S$  matrix calculated with the CH89 optical potential is represented by a (black) dash-dotted line, the (red) solid line shows the energy-dependent EST (eEST) separable representation of the  $S$  matrix, while the energy-independent EST separable representation is indicated by a (green) dashed line. The relative error is depicted by (red) circles for the eEST separable representation and by (green) upward triangles for the energy-independent EST construction. The EST support points are at  $E_{lab} = 16, 29$ , and  $47$  MeV.

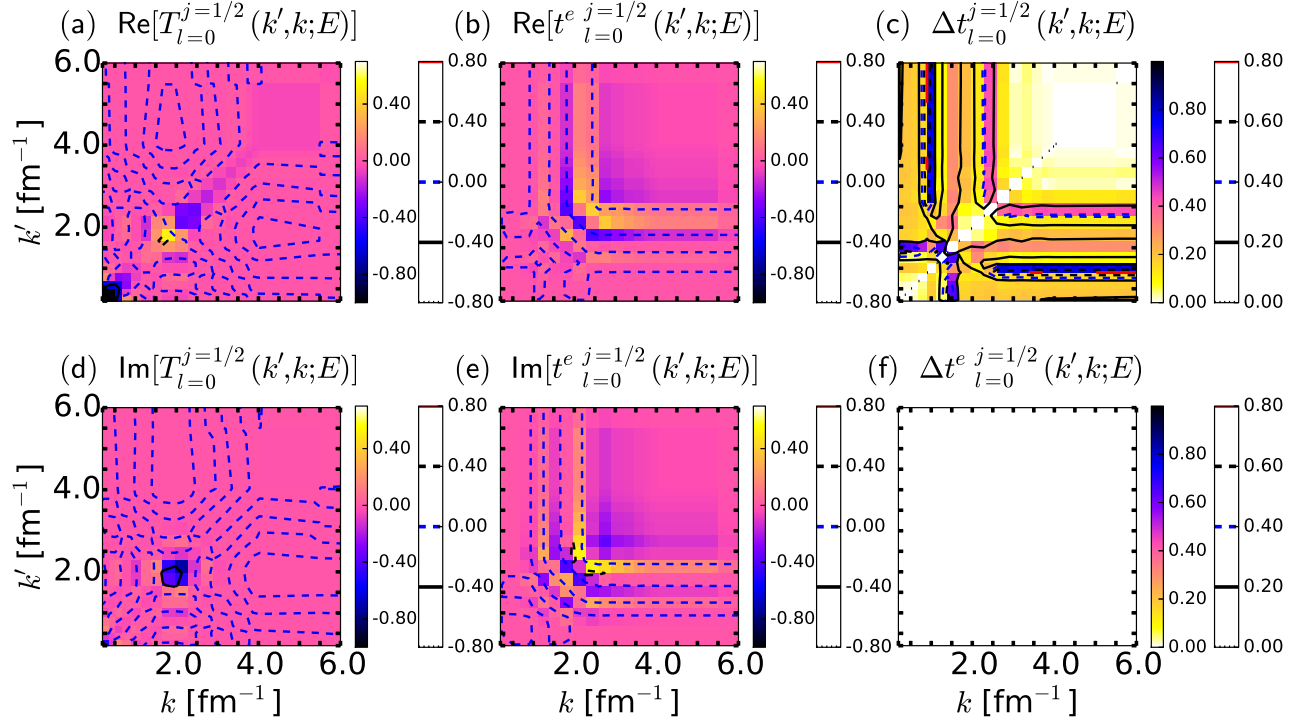


FIG. 5. (Color online) The  $l = 0, j = 1/2$  partial wave off-shell  $t$ -matrix elements,  $t_0(k', k; E)$  in units  $\text{fm}^2$  for the  $p+^{208}\text{Pb}$  system computed at  $E_{lab} = 21$  MeV as function of the off-shell momenta  $k'$  and  $k$ . This energy corresponds to an on shell momentum of  $1.00 \text{ fm}^{-1}$ . The real and imaginary parts of the off-shell  $t$  matrix calculated from the CH89 phenomenological optical potential are shown in panels (a) and (d). The real and imaginary parts of its eEST separable representation are depicted in panels (b) and (e). Panels (c) and (f) depict the asymmetry for the energy-independent EST and eEST separable representations. The calculated numbers in panel (f) are numerically zero, thus below the plot threshold and shown as white surface. The support points for the separable representation are at  $E_{lab}=5, 11, 21, 36$ , and  $47$  MeV.



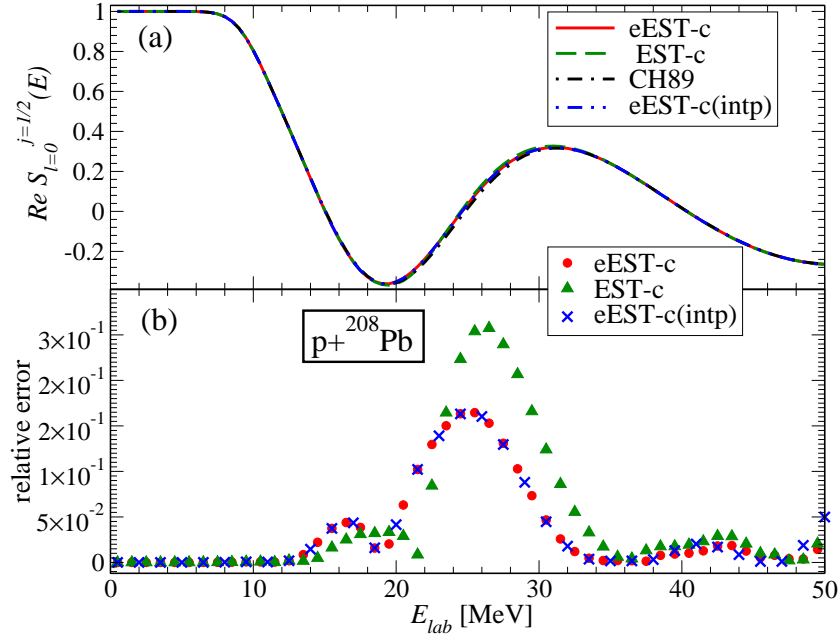


FIG. 6. (color online) The  $S$  matrix elements  $S_{l=0}^{j=1/2}(E)$  for elastic scattering of protons from  $^{208}\text{Pb}$  in the  $l=0, j=1/2$  partial wave as function of the laboratory energy. The top panel (a) shows the real part of the  $S$  matrix while the bottom panel (b) shows the relative error of the separable representations as defined in Eq. (21). The  $S$  matrix calculated from the CH89 phenomenological optical potential [21] is represented by a (black) dash-dotted line. The (red) solid line shows the energy-dependent EST (eEST-c) separable representation of the  $S$  matrix. The energy-independent EST separable representation (EST-c) is indicated by a (green) dashed line. The relative error is depicted by (red) circles for the eEST separable representation and by (green) upper triangles for the energy-independent EST construction. The EST support points for this case are  $E_{lab} = 5, 11, 36,$  and  $47$  MeV. The interpolated eEST separable representation (eEST(intp)-c) is shown by a (blue) dash-dot-dotted line. The corresponding relative error is shown by (blue) crosses. Cubic splines were employed for the interpolation of  $\mathcal{M}^c(E)$  on the grid  $E_{lab} = 5, 11, 36,$  and  $47$  MeV.